Bayesian Data-Analysis Toolbox
Release 4.23, Manual Version 3

G. Larry Bretthorst
Biomedical MR Laboratory
Washington University School Of Medicine,
Campus Box 8227
Room 2313, East Bldg.,
4525 Scott Ave.
St. Louis MO 63110
http://bayes.wustl.edu
Email: gbretthorst@wustl.edu

September 18, 2018

Chapter 10

Metabolic Analysis

The metabolic analysis package is designed to analyze Fids of a known type where one relates the resonance intensities to some metabolic parameters. For example, in the glutamate package we have a number of metabolic parameters that relate the rates at which carbon enters the metabolic cycles to the intensities of the various carbon resonances. The program, Bayes Metabolite, infers these metabolic parameters using a metabolic model to calculate the intensities of the metabolic resonances. The program takes as its input a nonarrayed Fid and a series of files that describe the metabolite and the nuisance resonances. A metabolite is the set of resonances who's intensities are predicted by the metabolic model. The nuisance resonances are all the other resonances in the data. Metabolites are described in a file having an ".ISO" suffix, and nuisance resonances are described in files suffixed with ".Res". For example, the example metabolite file is named "Example.ISO" while the example nuisance resonance file is named "Example.Res". The file format is the same for both metabolites and nuisance resonances. However, nuisance resonances use only the part of the file that describes the resonances, those parts of the file describing the metabolites are ignored. Consequently, a metabolic file may be used as a nuisance resonance file, but a nuisance resonance file may not be as used as a metabolite file. The metabolite files identify the subroutine that processes the metabolite, they describe the metabolic parameters, the coupling constants, and the resonances. Here, by describe we mean, these files specify the names of the parameters, their valid ranges, and the prior probability to be used for each parameter.

Using the Bayes Metabolite package involves several steps: First, the Fid must be loaded. Second, one must specify the model by loading the metabolite models and the nuisance resonance model. Third, the spectrum must be properly referenced so that all of the resonances in the model overlap the peaks in the spectrum of the Fid. Fourth, the metabolic parameters and the resonance frequencies must be reviewed to make sure that everything is correct. Finally, one runs the analysis and views the results using the standard widgets. We discuss each of these steps in more detail in the following paragraphs.

Select the Metabolite package from the Package menu.

Load the Fid to be analyzed using the Files menu. The loaded Fid will be displayed in the Fid Data Viewer.

Load the Metabolite file using the "Metabolite System" or the "Metabolite User" see Fig. 10.1.

Figure 10.1: The Bayes Metabolite Interface

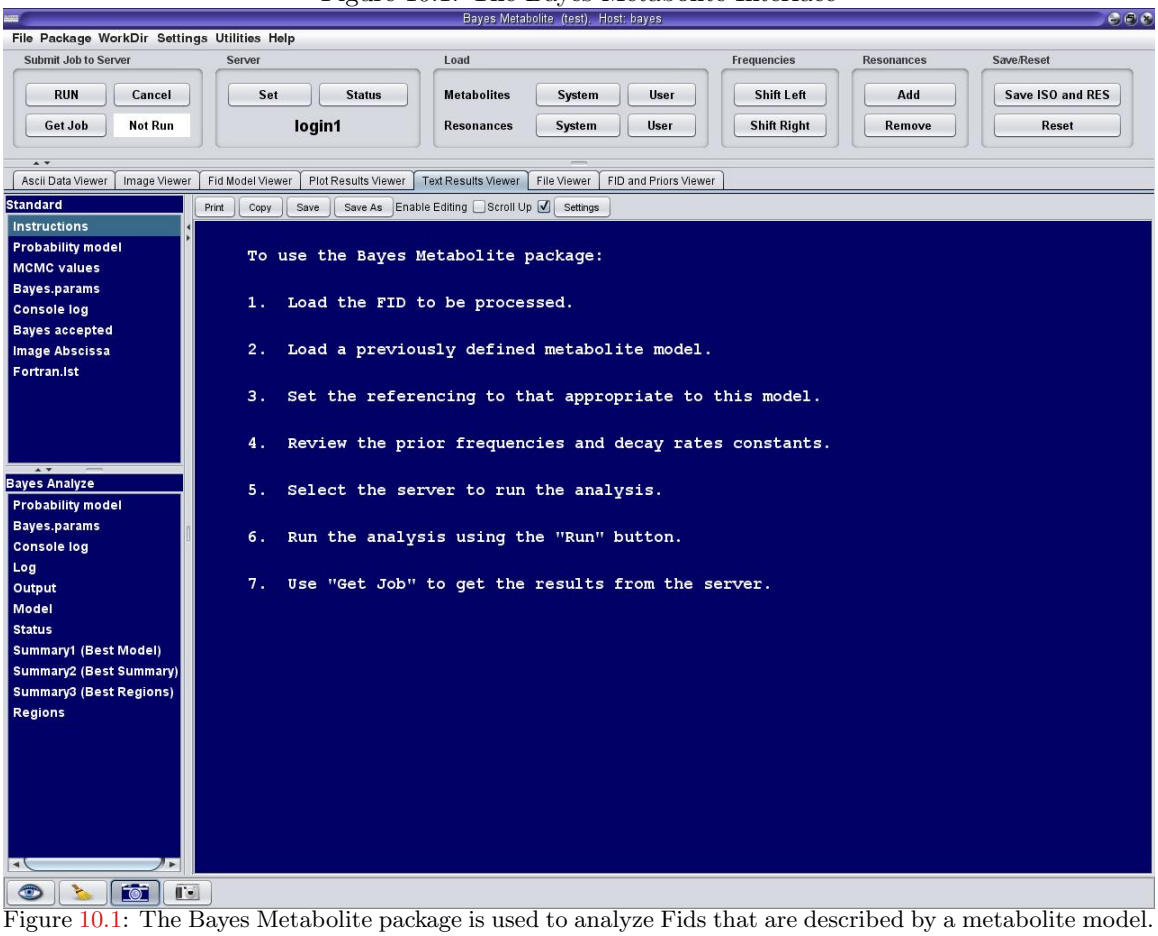

Figure 10.1: The Bayes Metabolite package is used to analyze Fids that are described by a metabolite model. To use the package, one loads the Fid, Loads the Metabolite and resonance models, shifts the resonance if necessary, and finally, runs the analysis.

Activating the "Metabolite System" button will bring up a list of Metabolite files on your specified server, while activating the "Metabolite User" button, will bring up a list of Metabolite files contained in your BayesHome directory: "BayesHome/Bayes.Predefined.Spec," where the BayesHome directory is where the Bayesian Analysis files are located in your home directory. This directory will be Bayes, unless you have changed it. In either case, select the metabolite file you wish to load and hit the "Open" button. In addition to loading the resonances from the metabolite file, opening the metabolite file will also copy the metabolite file to BayesHome/Bayes.Predefined.Spec directory. After loading the metabolite, the interface displays the Metabolite in a special Metabolite viewer, see Fig. 10.2. The Metabolite viewer can be used to shift blocks of resonances and it can be used to modify the prior ranges.

Load the Resonance file by activating either the "Resonance System" or the "Resonance User" buttons, see Fig. 10.1. These buttons function exactly the same as "Metabolite System" and User buttons, but these load resonance files, not metabolite files.

Examine each section of the spectrum and the model to make sure that the Metabolic and Resonance models are properly aligned. When aligning resonances, all displayed resonances are shifted in a block. To shift a block of resonances, use a double cursor. Place one cursor on the center of one of the peaks, and place the other cursor at the location you wish to shift that peak to. The "Shift Left" button assumes the right-hand cursor is the peak and it shifts the peak to the location of the left-hand cursor. Similarly, the "Shift Right" button assumes the left cursor is on the peak and shifts it to the location of the right cursor.

Review the metabolic and resonance parameters by clicking on their names on prior viewer. You can change any parameter range in a metabolite.

Select the server that is to process the analysis.

Check the status of the selected server to determine if the server is busy, change to another server if the selected server is busy.

Run the the analysis on the selected server by activating the Run button.

Get the the results of the analysis by activating the Get Job button. If the analysis is running, this button will return the Accepted report containing the status of the current run. Otherwise, it will fetch and display the results from the current analysis.

View the Bayes Metabolite model by activating "Fid Model Viewer." The Bayes Metabolite model Fid contains multiple traces. The first trace is the original data, the second is a model of the Fid produced from the parameter values that maximized the joint posterior probability for the parameters, and the third is the residuals (the difference between the data and the model). Each metabolite also outputs one trace for each site in each metabolite. For example, the Glutamate.2.0 metabolite model has 4 sites, so four additional output site traces are written. Each site trace contains all of the resonances in that site. When metabolite models were loaded all of the nuisance resonances are output in a single final trace. So the Glutamate.2.0 metabolite would output a total of $3 + 4 + 1 = 8$ traces. When no metabolite models are loaded, the nuisance resonances are output in individual traces.

Figure 10.2: The Bayes Metabolite Viewer

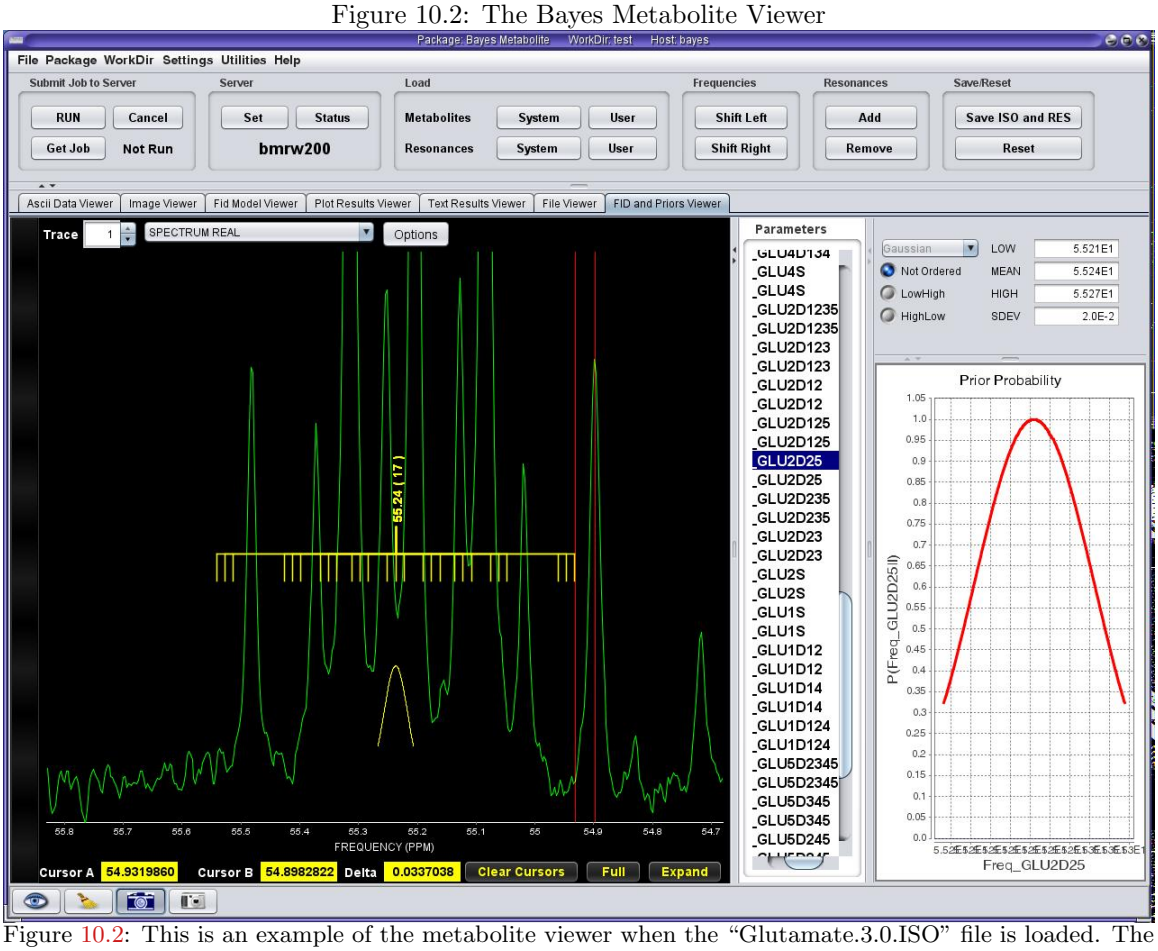

Figure 10.2: This is an example of the metabolite viewer when the "Glutamate.3.0.ISO" file is loaded. The left-hand portion of the viewer is the standard file viewer while the right-hand portion is an instance of the prior viewer. Using the file viewer one can align the spectrum and the model using the shift buttons. These buttons shift blocks of resonances either left or right by the amount of the double cursor. The prior viewer can be used to adjust and change the ranges of the various priors.

10.1 The Metabolic Model

The model used in Bayes Metabolite is of two parts, a metabolic model and a nuisance resonance model. These two models differ from each other in two important respects, nuisance resonance models have an amplitude associated with each resonance and they have no metabolic parameters; while metabolic models predict the fractional intensity of each metabolic resonance from the metabolic parameters. Thus metabolic models contain the chemistry, while nuisance resonances complete the spectral model.

Bayes Metabolite process a single non-arrayed Fid. Free induction decays consists of two data sets, a real data set and a quadrature or imaginary data set. These data sets are related to each other in the time domain model by a 90° phase shift. The time domain model of real data used in Bayes Metabolite is

$$d_R(t_i) = G_R(t_i) + n_i \tag{10.1}$$

where $d_R(t_i)$ represents the data acquired at time t_i, $G_R(t_i)$ represents the model of the data and n_i represents the misfit between the data and the model. The real data model is a sum of four terms:

$$G_R(t_i) \equiv F_R\delta(t_1 - t_i) + C_R + \sum_{j=1}^{m} M_{Rj}(t_i) + N_R(t_i), \tag{10.2}$$

these four terms are the first point model $F_R\delta(t_1 - t_i)$, a constant model C_R, the metabolic model represented by the sum, and finally the nuisance model $N_R(t_i)$. In NMR Fid data, it is not unusual for the first values to be in error by as much as a factor of two. Rather than discarding this data, this effect is included in the Fid model using a first point model. This is represented symbolically by $F_R\delta(t_1 - t_i)$ where F_R is related to the true intensity of the first point, and the delta function ensures this model is zero everywhere except the first data value. In addition to first point problems, it is also not unusual for the data to contain a constant offset. This is modeled by a constant C_R. Bayes Metabolite can process up to 4 different metabolic models at one time. The number of metabolic models being processed is m, where the jth metabolic model is represented by symbolically $M_{Rj}(t_i)$, and the nuisance resonance are represented by $N_R(t_i)$.

The metabolite model for the real data, $M_R(t_i)$, is a sum over each resonance in each isotopomer in the metabolic model,

$$M_R(t_i) = \sum_{\ell=1}^{N_B} B_\ell \sum_{k=1}^{n_\ell} F_{\ell k}(\Theta)\mathrm{R}(2\pi f_{\ell k}[t_i + t_0] + \phi_{\ell k}) \exp\{-\alpha_{\ell k} t_i\} \tag{10.3}$$

where we have represented the resonances symbolically by "RealRes". Metabolic resonances are grouped together by isotopomers or sites. For example, the kth resonance of the ℓth site might be a C2 doublet coming about from the J_{12} coupling in glutamate. The number of sites is designated as N_B and the number of resonances within the ℓth site is n_ℓ. The amplitude of each resonance is calculated from the total amplitude of the site, B_ℓ, and the fractional intensity, $F_{\ell k}$, of each site resonance. These fractional intensities are computed from the metabolite parameters Θ. The total fractional intensity of a given site sums to one, so

$$\sum_{k=1}^{n_\ell} F_{\ell k}(\Theta) = 1. \tag{10.4}$$

The frequency of the kth resonance of the ℓth site is denoted as $f_{\ell k}$, t_0 may be thought of as a linear or first order phase correction, and $\phi_{\ell k}$ is the constant part of the resonance phase. In this model each resonances decays exponentially. The exponential decay rate constant is represented by $\alpha_{\ell k}$. Note that if a resonances is a multiplet then all lines in a multiplet decay with the same exponential decay rate constant.

The resonance model, "RealRes," is a multiplet of multiplets of multiplets. We will use this resonance model for both metabolic and nuisance resonances. Consequently we will represent the frequency of the resonance as f_x where the x subscript could be both a site and resonances subscript as in the metabolic models, or it could be only a resonance subscript. The time domain model of a multiplets of multiplet of multiplets is given by

$$\mathrm{RealRes}(2\pi f_x[t_i + t_0] + \phi_x) \equiv \sum_{u=1}^{O_P} R_u^{O_P} \sum_{v=1}^{O_S} R_v^{O_S} \sum_{w=1}^{O_T} R_w^{O_T} \cos(2\pi \mathcal{F}_{uvw}[t_i + t_0] + \phi_x) \tag{10.5}$$

where the primary multiplet order is O_P, the secondary order is O_S, and O_T is the tertiary order. The fractional intensity of the uth line of the primary multiplet is $R_u^{O_P}$. Similarly, $R_v^{O_S}$ and $R_w^{O_T}$ are the fractional intensities of the various lines in the secondary and tertiary multiplets. The fractional intensities of for each multiplet sums to one, so

$$\sum_{u=1}^{O_P} R_u^{O_P} = 1, \qquad \sum_{v=1}^{O_S} R_v^{O_S} = 1 \quad \text{and} \quad \sum_{w=1}^{O_T} R_w^{O_T} = 1; \tag{10.6}$$

then by definition the fractional intensity of the various lines in the multiplet of multiplets of multiplets must sum to one:

$$\sum_{u=1}^{O_P} \sum_{v=1}^{O_S} \sum_{w=1}^{O_T} R_u^{O_P} R_v^{O_S} R_w^{O_T} = 1. \tag{10.7}$$

The interface defaults these fractional intensities to spin one half multiplets. However, these fractional intensities are input from the interface and may be changed by the user. Finally, the frequency, $\mathcal{F}_{uvw}$, is given by

$$\begin{aligned} \mathcal{F}_{uvw} &= \mathcal{F}_{uv} - \frac{J_T(O_T + 1 - 2w)}{2}, \\ \mathcal{F}_{uv} &= \mathcal{F}_u - \frac{J_S(O_S + 1 - 2v)}{2}, \\ \mathcal{F}_u &= f_x - \frac{J_P(O_P + 1 - 2u)}{2} \end{aligned} \tag{10.8}$$

where J_P, J_S and J_T are the primary, secondary and tertiary coupling constants in Hertz and f_x is the center frequency of the multiplet in Hertz. Note that the package actually uses PPM as its units for the center frequency, so the program converts the frequency, f_x, to Hertz prior to using these formula.

The nuisances resonance model, $N_R(t_i)$, is defined as

$$N_R(t_i) \equiv \sum_{k=1}^{n} B_k \mathrm{RealRes}(2\pi f_k[t_i + t_0] + \phi_k) \exp\{-\alpha_k t_i\} \tag{10.9}$$

where B_k is the amplitude of the kth resonance. The other quantities appearing in this equation have the same meaning as those defined in Eq. (10.5), except here they refer to the nuisance resonances.

The time domain the data consists of a real and a quadrature or imaginary data. The imaginary data are modeled as

$$d_I(t_i) = G_I(t_i) + \text{Noise} \tag{10.10}$$

with

$$G_I(t_i) \equiv F_I\delta(t_1 - t_i) + C_I + \sum_{j=1}^{m} M_{Ij}(t_i) + N_I(t_i) \tag{10.11}$$

where $d_I(t_i)$ represents the imaginary data at time t_i, F_I is the first point model, C_I is the constant offset, $M_{Ij}(t_i)$ is the jth metabolic model, $N_I(t_i)$ are the nuisance resonances, and "Noise" represents the misfit between the data and the model in the imaginary data. Note that "Noise" is only a symbolic representation of this misfit and should not be taken to mean that the noise is the same in the real and imaginary data.

The imaginary metabolic model, $M_I(t_i)$, is just a 90° phase shifted version of the real metabolic model and is given by

$$M_I(t_i) = \sum_{\ell=1}^{N_B} B_\ell \sum_{k=1}^{n_\ell} F_{\ell k}(\Theta)\text{ImagRes}(2\pi f_{\ell k}[t_i + t_0] + \phi_{\ell k}) \exp\{-\alpha_{\ell k} t_i\} \tag{10.12}$$

where

$$\text{ImagRes}(2\pi f_k[t_i + t_0] + \phi_k) \equiv -\sum_{u=1}^{O_P} R_u^{O_P} \sum_{v=1}^{O_S} R_v^{O_S} \sum_{w=1}^{O_T} R_w^{O_T} \sin(2\pi \mathcal{F}_{uvw}[t_i + t_0] + \phi_x). \tag{10.13}$$

All of the quantities within these equations are the same as those defined for the real channel. Similarly, The nuisances resonance model for the imaginary data, $N_I(t_i)$, is defined as

$$N_I(t_i) \equiv \sum_{k=1}^{n} B_k \text{ImagRes}(2\pi f_k[t_i + t_0] + \phi_k) \exp\{-\alpha_k t_i\}. \tag{10.14}$$

10.2 The Bayesian Calculation

The calculation performed by Bayes Metabolite is for the marginal posterior probability for each parameter appearing in the model. If we designate all of the parameters appearing in the model, except the standard deviation of the noise prior probability, as χ, then the marginal probability for χ_j is given by

$$P(\chi_j|DI) \propto \int d\chi_1 \ldots d\chi_{j-1} d\chi_{j+1} \cdots d\chi_z P(\chi|DI) \tag{10.15}$$

where all of these integrals are evaluated numerically. The posterior probability for each of the parameters may be computed from joint posterior probability, $P(\chi|DI)$, and it is this distribution that is targeted by the Markov chain Monte Carlo simulations.

The joint posterior probability for the parameters is a marginal probability where the standard deviation of the noise has been removed analytically:

$$P(\chi|DI) \propto \int d\sigma P(\chi\sigma|DI) \tag{10.16}$$

where $P(\chi\sigma|D\sigma I)$ is the joint posterior probability for all of the parameters. To compute this probability one applies Bayes' theorem to obtain

$$P(\chi|DI) \propto \int d\sigma P(\chi\sigma|I)P(D|\chi\sigma I). \tag{10.17}$$

In the preceding we are using D to stand for both the real and imaginary data. If we designate D_R and D_I as the real and imaginary data, then the joint posterior probability is given by

$$P(\chi|DI) \propto \int d\sigma P(\chi|I)P(\sigma|I)P(D_R|\chi\sigma I)P(D_I|\chi\sigma I). \tag{10.18}$$

We used logical independence to factor both the joint prior probability and the likelihood. The joint prior probability was factored into a prior probability for the standard deviation of the noise, $P(\sigma|I)$, and the joint prior probability for all of the other parameters $P(\chi|I)$. The joint likelihood for the data, $P(D_R D_I|\chi\sigma I)$, was factored into independent likelihood for each data set separately.

If we assign the prior probability for the noise standard deviation using a Jeffreys' prior, and assign the two likelihoods, $P(D_R|\chi\sigma I)$ and $P(D_I|\chi\sigma I)$, using a Gaussian prior probability, one obtains

$$P(\chi|DI) \propto \int P(\chi|I)d\sigma \frac{1}{\sigma}\left(2\pi\sigma^2\right)^{-N} \exp\left\{-\frac{Q_R+Q_I}{2\sigma^2}\right\} \tag{10.19}$$

with

$$Q_R = \sum_{i=1}^{N}\left[d_R(t_i) - G_R(t_i)\right]^2 \tag{10.20}$$

where N is the total complex data values, and

$$Q_I = \sum_{i=1}^{N}\left[d_I(t_i) - G_I(t_i)\right]^2. \tag{10.21}$$

Evaluating the integral over the standard deviation, one obtains

$$P(\chi|DI) \propto P(\chi|I)\left[Q_R + Q_I\right]^{-N} \tag{10.22}$$

where we have dropped some constants that cancel on normalization.

The joint prior probability for the other parameters is factored into independent prior probability for each parameter

$$\begin{aligned} P(\chi|I) &= P(F_R|I)P(F_I|I)P(C_R|I)P(C_I|I)P(t_0|I)P(\phi|I) \\ &\times \left[\prod_{k=1}^{N_J} P(J_k|I)\right]\left[\prod_{k=1}^{n} P(B_k|I)P(f_k|I)P(\alpha_k|I)P(\phi_k|I)\right] \\ &\times \prod_{j=1}^{m}\left\{\left[\prod_{k=1}^{N_{\Theta j}} P(\Theta_{jk}|I)\right]\left[\prod_{k=1}^{N_{Jj}} P(J_{jk}|I)\right]\left[\prod_{k=1}^{N_{Bj}} P(B_{jk}|I)\right]\right. \\ &\times \left.\left(\prod_{\ell=1}^{N_{Bj}}\left[\prod_{k=1}^{n_{j\ell}} P(f_{j\ell k}|I)P(\alpha_{j\ell k}|I)P(\phi_{j\ell k}|I)\right]\right\}\right) \end{aligned} \tag{10.23}$$

Figure 10.3: Bayes Metabolite Parameters And Probabilities List

Parameter	Description	
N_J:	The number of J coupling constants in the nuisance model	
n:	The number of resonances in the nuisance model	
$N_{\Theta j}$:	The number of metabolic parameter in the jth metabolite	
N_{Jj}:	The number of J coupling constants in the jth metabolite	
N_{Bj}:	The number of sites/amplitudes in the jth metabolite	
$n_{\ell j}$:	The number of resonances in the ℓth site of the jth metabolite	
Prior Probability	Description of the Global Parameters	Assigned
$P(F_R\|I)$:	the real first point offset	Gaussian
$P(F_I\|I)$:	the imaginary first point offset	Gaussian
$P(C_R\|I)$:	the real constant offset	Gaussian
$P(C_I\|I)$:	the imaginary constant offset	Gaussian
$P(\phi\|I)$:	the constant part of the resonance phase	uniform
$P(t_0\|I)$:	the time offset, i.e., linear frequency dependent phase	Gaussian
Prior Probability	Description of the Nuisance Resonances Parameters	Assigned
$P(J_k\|I)$:	the kth J coupling constant	user input
$P(B_k\|I)$:	the amplitude of the kth resonance	Gaussian
$P(f_k\|I)$:	the frequency of the kth resonance	user input
$P(\alpha_k\|I)$:	the decay rate constant of the kth resonance	user input
$P(\phi_k\|I)$:	the constant phase of the kth resonance	user input
Prior Probability	Description of the Metabolic Parameters	Assigned
$P(\Theta_{jk}\|I)$:	the kth metabolic parameter in the jth metabolite	user input
$P(J_{jk}\|I)$:	the kth coupling constant in the jth metabolite	user input
$P(B_{jk}\|I)$:	the kth amplitude in the jth metabolite	Gaussian
$P(f_{j\ell k}\|I)$:	the frequency of the kth resonance, ℓth site, jth metabolite	user input
$P(\alpha_{\ell jk}\|I)$:	the decay rate of the kth resonance, ℓth site, jth metabolite	user input
$P(\phi_{jk}\|I)$:	the phase of the kth resonance, ℓth site, jth metabolite	user input

where we define the symbols and probabilities appearing in this equation in Table 10.3. In this table "user input" means that the information needed to assign the prior is read from the input parameter files. Prior probabilities assigned in this way are either bounded uniform or Gaussian prior probabilities. In both cases the user must specify all of the information necessary to assign the prior. Prior probabilities noted as being "Gaussians" are bounded zero mean Gaussian prior probabilities and the bound and standard deviations of these Gaussians are set by Bayes Metabolite. For example, the range for the amplitudes extends from zero to a few times the maximum data value and this range represents a 3 standard deviations interval; so the prior keeps the amplitudes positive and in a range that is reasonable for the data. The prior probability for the phases, the $P(\phi_{jk}|I)$ and the $P(\phi_k|I)$, are assigned as delta functions:

$$P(\phi_{jk}|I) = \delta(\phi - \phi_{jk}), \qquad \text{and} \qquad P(\phi_k|I) = \delta(\phi - \phi_k), \tag{10.24}$$

if the resonances has a common constant phase, and they are assigned a uniform prior probabilities if the resonance has a unique phase. Whether or not the resonance has a common phase is defined in the parameter files.

Markov chain Monte Carlo using simulated annealing is used to draw samples from Eq. (10.22). From these samples the marginal posterior probability for each parameters is generated. These posterior probabilities are written to an output files contained within the experiment. Additionally, the mean and standard deviation estimates of the parameters are written to mcmc.values file contained in the experiment. Finally, the parameters that maximized the joint posterior probability for the parameters are used to generate a model of the original Fid. This model may then be viewed using the appropriate interface widgets.

10.3 The Metabolite Models

Metabolic models consist of three parts: First, there must be a physical model of some chemical process. This physical model must lead to a prediction of the fractional intensities of the resonances in the spectrum. Second, a subroutine must use this physical model to compute the fractional intensities of each resonance from the metabolic parameters. Finally, the metabolic and resonance parameters must be described to the program that processes the metabolite. In the following subsections we will describe the current metabolites, and then in the next Section we will give detailed instructions on how to build and test your own metabolic models.

10.3.1 The IPGD_D2O Metabolite

The methodology used for the estimates of the contribution of glycogenolysis, glycerol, and PEP to serum glucose was first proposed by Landau [19], with analysis of ^{2}H enrichment carried out by mass spectroscopy. How this labeling is carried out is illustrated symbolically in Fig. 10.4. Peak intensities from the H2, H5, H6S and H6R resonances are used to calculate the contribution of Glycogen, Glycerol and the Kreb's cycle to the creation of Glucose. The three contributions are computed from the H2, H5 and H6 intensities. The H6 intensity is either H6R or H6S. Ratios are computed using H6R intensities to make sure that nothing has gone wrong in the experiment; it is the ratios computed using the H6S intensities that are of metabolic importance.

Data typical of this metabolic model are shown in Fig. 10.5. For this work, the samples of serum glucose were prepared according to Jones, et. al. [34]. Deuterium NMR spectroscopy was carried out at 92Mhz. The 90 degree pulse width was 7.9us. The spectral width was set to 10ppm and 928 data points were collected in the Fid to give a total acquisition time of 1s with no further relaxation delay. The longest relaxation time for a deuteron in the IPG derivative is 230ms.

The four resonances used in the metabolic calculations are labeled H2, H5, H6R and H6S respectively. The remaining resonances, including the solvent peaks are described by the IPGD_D2O.Res file. In this simple metabolite, the metabolic parameters *are* the fractional intensities of the H2, H5, H6R and H6S resonances. Because the total fractional intensity must add up to one, we impose the condition

$$1 = \mathrm{H2} + \mathrm{H5} + \mathrm{H6}_R + \mathrm{H6}_S. \tag{10.25}$$

From the fractional intensities there are six derived parameters that are output from the IPGD_D2O

Figure 10.4: The IPGD_D20 Metabolite

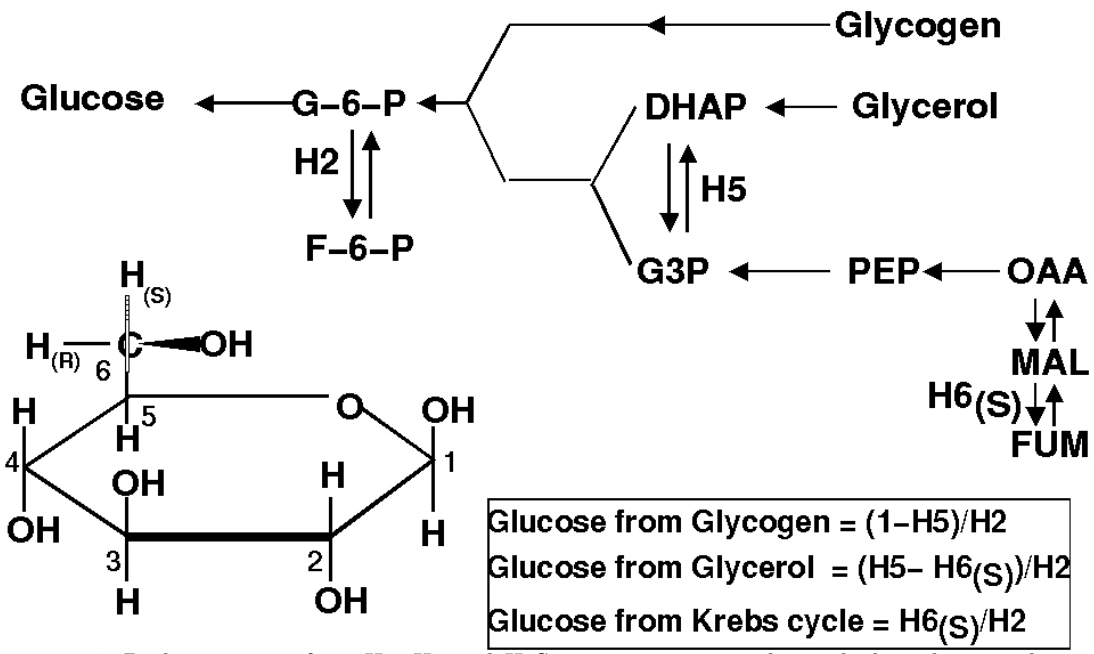

Figure 10.4: Peak intensities from H2, H5 and H6S resonances are used to calculate the contribution of Glycogen, Glycerol and the Kreb's cycle to the creation of Glucose, see [34]. This figure courtesy of John G. Jones, South Western Medical Center.

Figure 10.5: Bayes Metabolite IPGD_D20 Spectrum

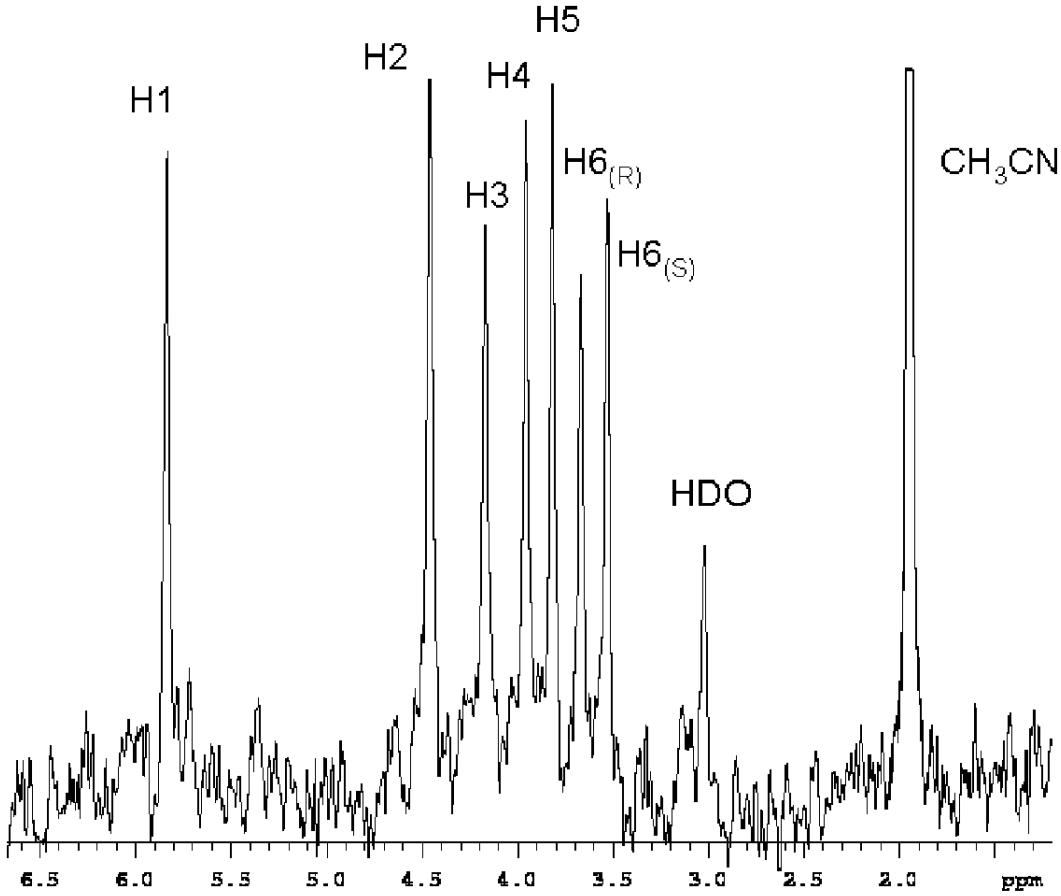

Figure 10.5: This spectrum is a typical example of IPGD_D2O data. It is the ratios, as described in the text, of the labeled four peak that are computed by the IPGD_D2O metabolic package. Note the four metabolic peaks of interest have been annotated. The remaining resonances, including the solvent, are described by the IPGD_D2O.Res file and are the intensities of these peaks are not used in the Metabolic analysis.

Figure 10.6: The Fraction Of Glucose From Glycogenolysis, Glycerol And The Krebs Cycle

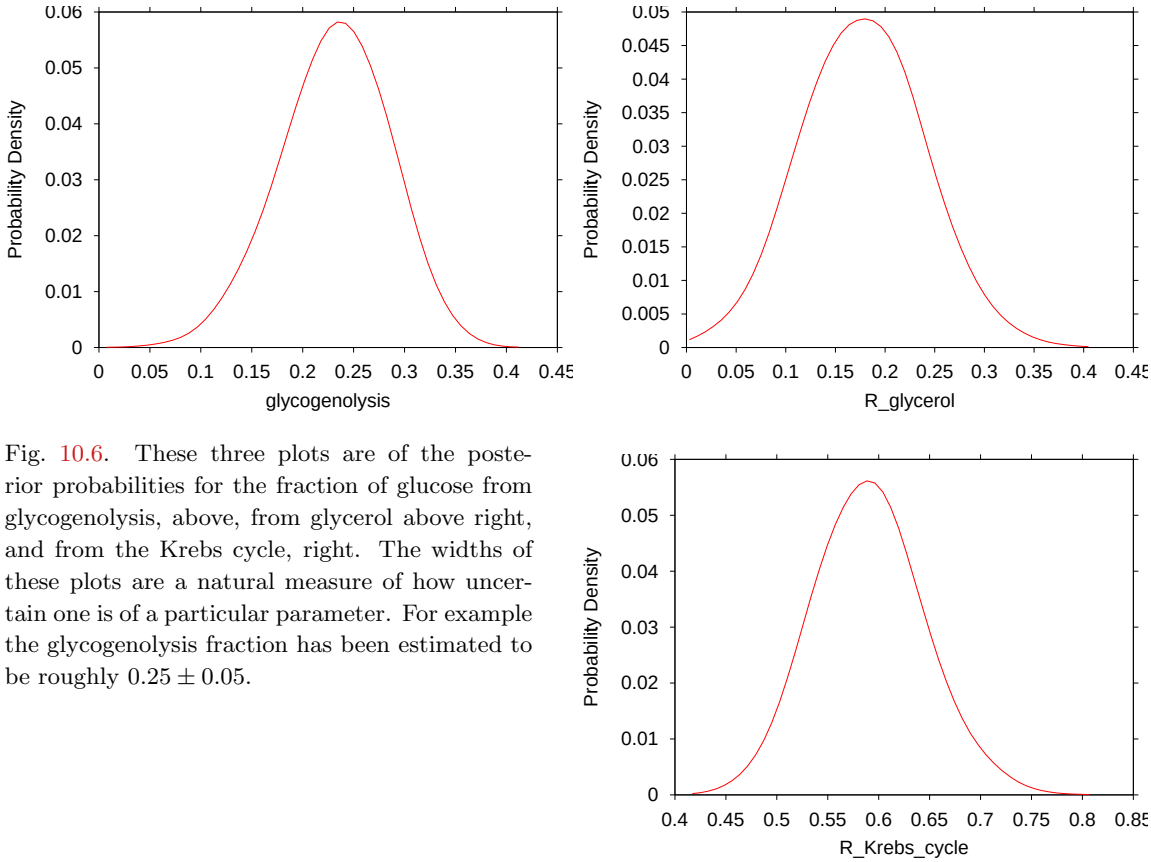

Fig. 10.6. These three plots are of the posterior probabilities for the fraction of glucose from glycogenolysis, above, from glycerol above right, and from the Krebs cycle, right. The widths of these plots are a natural measure of how uncertain one is of a particular parameter. For example the glycogenolysis fraction has been estimated to be roughly 0.25 ± 0.05.

metabolite analysis:

$$\begin{aligned}
\text{Spins_H2} &= \text{H2}, \\
\text{glycogenolysis} &= 1 - \frac{\text{H5}}{\text{H2}}, \\
\text{R_glycerol} &= \frac{\text{H5}-\text{H6}_{(R)}}{\text{H2}}, \\
\text{R_Krebs_cycle} &= \frac{\text{H6}_{(R)}}{\text{H2}}, \\
\text{S_glycerol} &= \frac{\text{H5}-\text{H6}_{(S)}}{\text{H2}}, \\
\text{S_Krebs_cycle} &= \frac{\text{H6}_{(S)}}{\text{H2}}.
\end{aligned} \tag{10.26}$$

Using the data shown in Fig. 10.5, and the IPGD_D2O.ISO and IPGD_D2O.Res files we ran this analysis and have displayed probability density functions for the three ratios of interest, the "S"

ratios, are shown in Fig. 10.6. For more on these calculations and why they are important see [34].

10.3.2 The Glutamate.2.0 Metabolite

The Glutamate 2.0 metabolic model is a model of the TCA cycle in hearts. This model was first proposed by Jeffrey, et. al. [42]. The assumption included in this model necessitate that only the perfusion described in Jeffrey, et. al. be utilized. Carbon-13 spectroscopic analysis of the glutamate isotopomer can be carried out on the unpurified abstract of the freeze clamped heart, with two caveats. The spectroscopy should be at 100 MHz carbon frequency or above to minimize second order effects in the multiplets, and the relaxation delay should be 2.5s with a 90 degree excitation pulse so that different resonances are not weighted by relaxation effects. A spectrum typical of this experiment is displayed in Fig. 10.7. The four panels in this figure are the resonances that each of the four carbon isotopomer gives rise to. The function of the Glutamate metabolic model is to predict the relative intensity of each of the resonances within each isotopomer.

For a heart perfused with [2-^{13}C] acetate plus [3-^{13}C] propionate, there are three basic metabolite parameters:

- F_{c2}: The fraction of acetyl-CoA enriched in C2.
- y: Anaplerosis, Carbon skeleton entry into the TCA acid cycle relative to citrate synthase; by definition $y \geq 0$.
- F_{a1}: Anaplerotic substrate enriched in a single aliphatic carbon.

From these three parameters, there are two derived parameters:

- F_{c0}: By definition if F_{c2} is the fraction of acetyl-CoA enriched in C2, and F_{c0} is the fraction not enriched, then
$$F_{c0} + F_{c2} = 1. \tag{10.27}$$
- F_{a0}: Similarly if F_{a1} is the Anaplerotic substrate enriched in aniphatic carbon, and F_{a0} is the fraction not enriched, then
$$F_{a0} + F_{a1} = 1. \tag{10.28}$$

These five metabolic parameters are used by the Glutamate.2.0 subroutine to predict the relative intensity of each resonance. In the process of computing the joint posterior probability for the model, the simulations will propose a set of metabolic parameters. These are passed to the Glutamate.2.0 subroutine, and that subroutine passes back the predicted relative amplitudes of each resonance in the model.

The Glutamate.2.0 model contains 11 resonances which interact through three coupling constants:

- J_{12}: The coupling constant between the C1 and C2 carbons,
- J_{23}: The coupling constant between the C2 and C3 carbons,
- J_{34}: The coupling constant between the C3 and C4 carbons.

Figure 10.7: Glutamate Example Spectrum

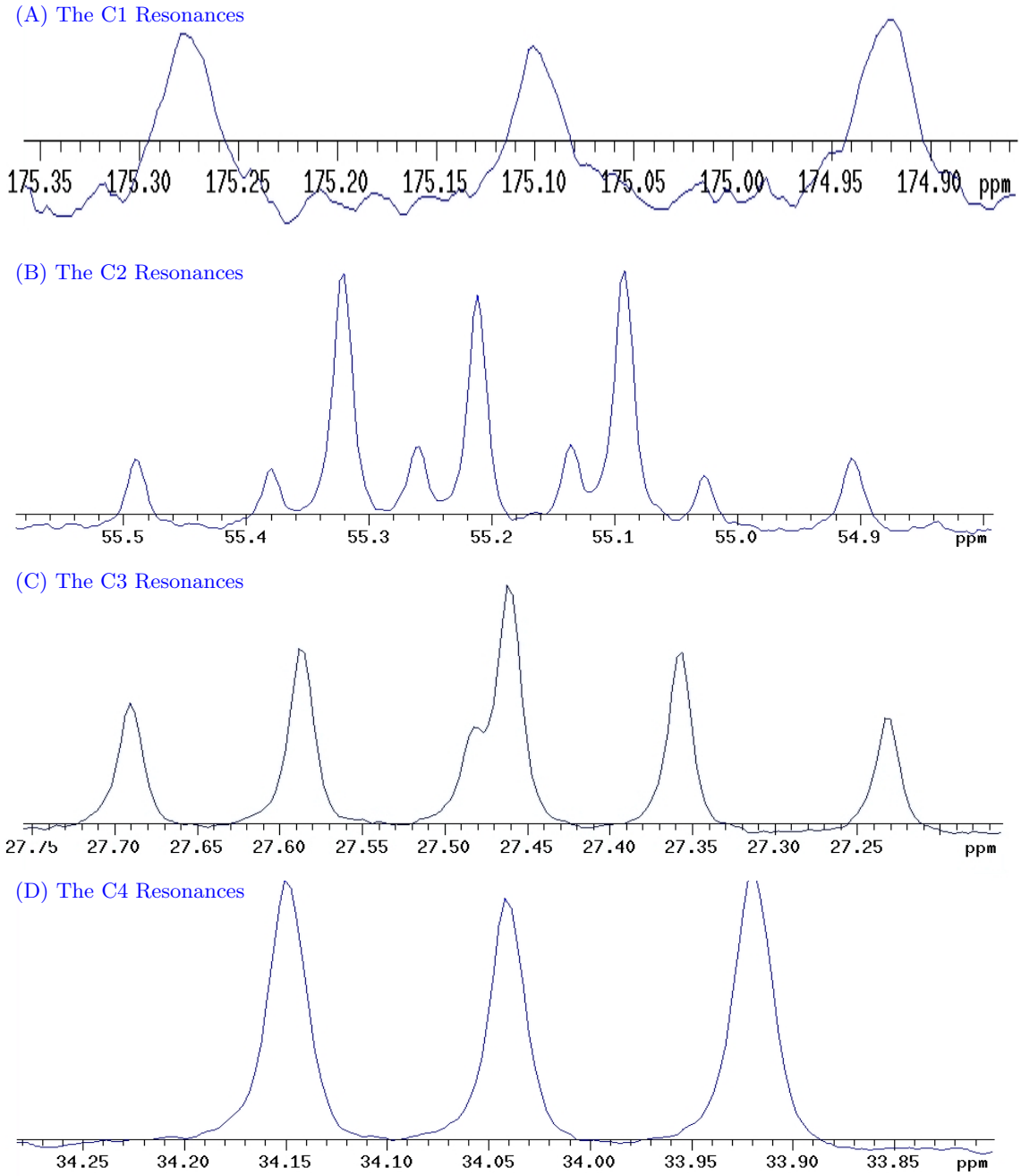

Figure 10.7: This spectrum is a typical example of Glutamate data: C1 is a singlet and a doublet; C2 is a doublet of doublets, two doublets and a singlet; C3 is a doublet of doublets, a doublet, and a singlet; finally, C4 is a doublet and a singlet.

The prior ranges, means, and standard deviations of these coupling constants are read from the "Glutamate.2.0.ISO" file. For example the J_{12} coupling constant is 54 ± 1 Hertz, with a low and high of 52 and 56 Hertz respectively. Typically these coupling constants are determined to better than 0.01 Hertz, so the priors have little effect on the numerical simulations; they serve only to make sure that the Markov chain keeps these coupling constants near the values supported by the data.

In the Glutamate.2.0 model there are four sites and so four amplitudes that must be estimated. The Glutamate.2.0 subroutine computes the normalized intensity of each resonance within each sites from the metabolic parameters. The four sites are named C1, C2, C3 and C4. So when we say that the Glutamate.2.0 subroutine must compute the fractional intensity of a sites we mean that each carbon gives rise to a set of related lines and total amplitude of an sites times the fractional intensity of a given resonance is equal to the intensity of that resonance.

These four carbons give rise to a total of 11 resonances. Figure 10.7 shows the resonances from each of the four carbons. These resonances are named Cn_x where Cn is the carbon giving rise to the resonance, and x designates which resonance. For example, $\mathrm{C2}_{d_{23}}$, is the C2 doublet caused by the J_{23} coupling. As noted, the Glutamate.2.0 subroutine must compute the fractional intensity of each resonance from the metabolic parameters. If we define

$$a = \frac{1}{y+1}, \tag{10.29}$$

$$b = \frac{1}{2(y+1)^2}, \tag{10.30}$$

and

$$c = bF_{c2} \tag{10.31}$$

then the fractional intensities for the two C1 resonances, shown in Fig. 10.7(A), are given by:

$$\begin{aligned} \mathrm{C1}_d &= aF_{c2}, \\ \mathrm{C1}_s &= 1 - \mathrm{C1}_d \end{aligned} \tag{10.32}$$

where $\mathrm{C1}_d$ is the fractional intensity of the C1 doublet due to J_{12} coupling and $\mathrm{C1}_s$ is the fractional intensity of the C1 singlet. Note, by definition $\mathrm{C1}_d + \mathrm{C1}_s = 1$.

Similarly, the fractional intensities of the four C2 resonances, shown in Fig. 10.7(B), are given by

$$\begin{aligned} \mathrm{C2}_{d_{23}} &= c(2y + F_{c0} + 1), \\ \mathrm{C2}_{d_{12}} &= cF_{c0}, \\ \mathrm{C2}_q &= cF_{c2}, \\ \mathrm{C2}_s &= 1 - \mathrm{C2}_{d_{12}} - \mathrm{C2}_{d_{23}} - \mathrm{C2}_q \end{aligned} \tag{10.33}$$

where $\mathrm{C2}_{d_{23}}$ is the fractional intensity of the C2 doublet due to J_{23} coupling, $\mathrm{C2}_{d_{12}}$ is the fractional intensity of the C2 doublet due to J_{12} coupling, $\mathrm{C2}_q$ is the fractional intensity of the C2 doublet of doublets due to J_{12} and J_{23} couplings, Finally, $\mathrm{C2}_s$ is the fractional intensity of the C2 singlet; and, as with the C1 resonances, the fractional intensity of the C2 singlet is computed in such a way as to insure $1 = \mathrm{C2}_{d_{12}} + \mathrm{C2}_{d_{23}} + \mathrm{C2}_q + \mathrm{C2}_s$.

The fractional intensities of the three C3 resonances, shown in Fig. 10.7(C), are given by

$$\begin{aligned} \mathrm{C3}_d &= C1_d(y + 2F_{c0}), \\ \mathrm{C3}_t &= C1_d F_{c2}, \\ \mathrm{C3}_s &= 1 - \mathrm{C3}_d - \mathrm{C3}_t \end{aligned} \tag{10.34}$$

where $\mathrm{C3}_d$ is the fractional intensity of the C3 doublet due to J_{23} coupling, $\mathrm{C3}_t$ is the fractional intensity of the C3 doublet of doublets due to J_{23} and J_{34} couplings. Note this doublet of doublet is often called a triplet because the coupling is such that the resonance pattern looks like a 1:2:1 triplet. Finally, $\mathrm{C3}_s$ is the fractional intensity of the C3 singlet, and as with the C1 and C2 resonances its intensity is computed in such a way as to insure $1 = \mathrm{C3}_d + \mathrm{C3}_t + \mathrm{C3}_s$.

The fractional intensities of the two C4 resonances, shown in Fig. 10.7(D), are given by

$$\begin{aligned} \mathrm{C4}_{d_{34}} &= (F_{c2} + yF_{A1})/(2y + 1) \\ \mathrm{C4}_s &= 1 - \mathrm{C4}_{d_{34}} \end{aligned} \tag{10.35}$$

where $\mathrm{C4}_{d_{34}}$ is the fractional intensity of the C4 doublet due to J_{34} coupling, and $\mathrm{C4}_s$ is the the fractional intensity of the C4 singlet.

To use the glutamate model, load the "Glutamate.2.0.ISO" isotopomer file and reference the C1 singlet to 175.1 ppm. Next hit the display spectrum button and the interface will note the locations of all of the prior probabilities on the spectrum. These priors should now overlap the centers of the C1 resonances. If they don't then you must not have gotten the referencing correct or something is wrong with the spectrum. Next expand the various regions of the spectrum and make sure that the priors overlap the centers of each of the carbon resonances. If they do not overlap, and you have referenced the spectrum, you will have to use the edit metabolic resonances button to correct the frequency shifts. Note that you must be careful in doing this to make sure that the resonances remain in the given order. This can be difficult, because the interface orders the priors by frequency, and if you change a frequency, you can change the order. If the order changes from what is coded into the glutamate subroutine, the Metabolite program will not even try to run. After making sure the resonances all line up, load the nuisance resonances. These nuisance resonances are in the "Glutamate.2.o.Res" file. This particular file was set up for the "sb33_90A.fid" located in the Bayes.test.data directory downloaded from the interface. If the nuisance resonances in your data set are different, unload the resonance file and use the edit parameters button under the processing type resonance label to enter the nuisance resonances. The easiest way to do this is simply to mark them using the buttons on the edit resonances window. Finally, run the analysis using the "Run Analysis" button.

10.3.3 The Glutamate.3.0 Metabolite

The newest metabolite to be added to the metabolite package is an extension of the glutamate 2.0 metabolite to account for the C5 couplings. This is an extensive addition to the metabolite package having some 19 metabolic parameters, 6 coupling constants and 27 sets of resonances. These resonances range from singlets to doublets of doublets of doublets. If you need more information on this metabolite consult the paper [41] and if this does not answer you questions contact its creator, Mark Jeffrey, at the Southwest medical center in Dallas Texas.

Figure 10.8: Estimating The F_{c0}, y and F_{a0} Parameters

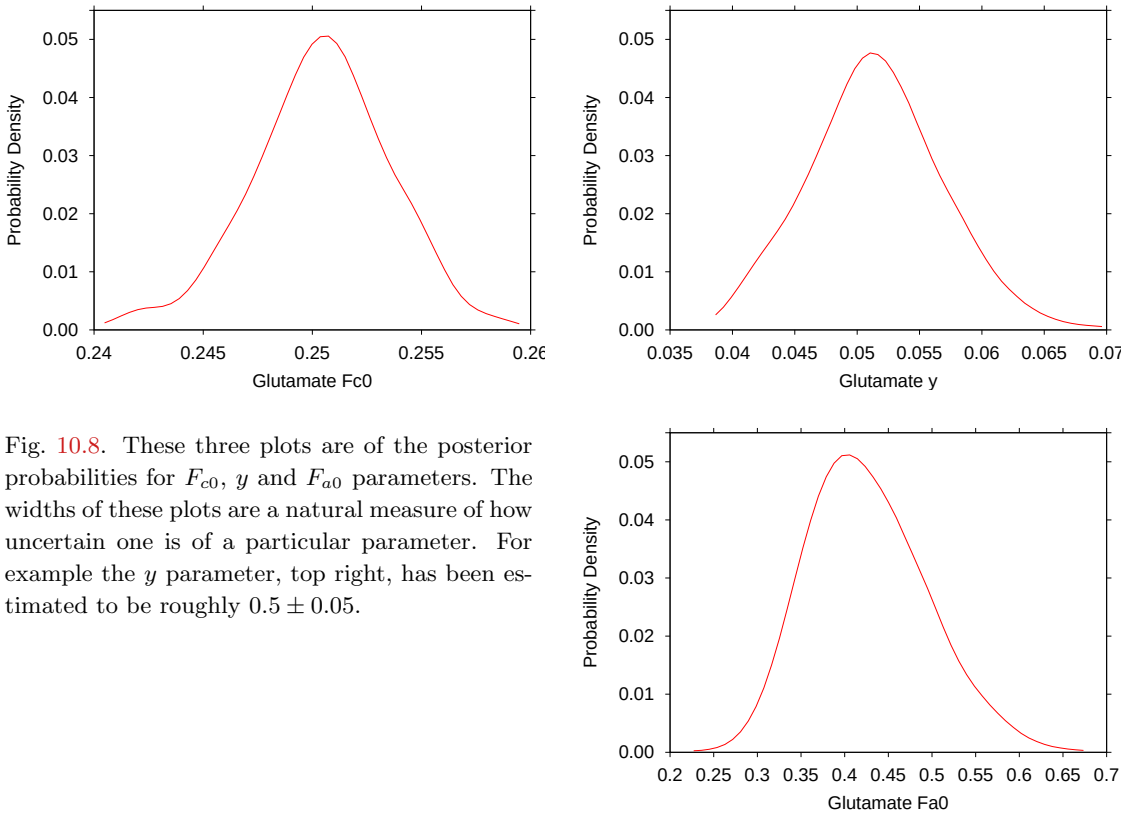

Fig. 10.8. These three plots are of the posterior probabilities for F_{c0}, y and F_{a0} parameters. The widths of these plots are a natural measure of how uncertain one is of a particular parameter. For example the y parameter, top right, has been estimated to be roughly 0.5 ± 0.05.

10.4 The Example Metabolite

The example metabolite is just what its name implies, its a simple example of a metabolite used to demonstration how to build metabolite model. This metabolite imposes only a single condition on the data, in this case it forces the fractional amplitudes of two multiplets to be in a fixed ration. The data used in the example is the "ethyl.ether.fid" and may be loaded from the Bayes.test.data directory. The spectrum of this data is shown in Fig. 10.9(A). To run the example metabolite, load the Fid, the "Example.ISO" file and the nuisance resonance file "Example.Res" and run the analysis.

The example metabolite only runs a few minutes. It has one metabolite and one derived parameter. In this case it is the fractional intensity of the triplet that is the metabolite parameters, the derived parameter is the fractional intensity of the quartet. The output from this metabolite is the two fractional intensities, the total intensity, the coupling constant, and the parameters needed to describe both the metabolite and nuisance resonances. These outputs may be viewed using the standard widgets. Additionally, the metabolite model generated from the maximum posterior probability estimate of the parameters may be viewed by activating the Fid model viewer. see Section **??** for more on how to use the model experiment.

Figure 10.9: Bayes Metabolite, The Ethyl Ether Example

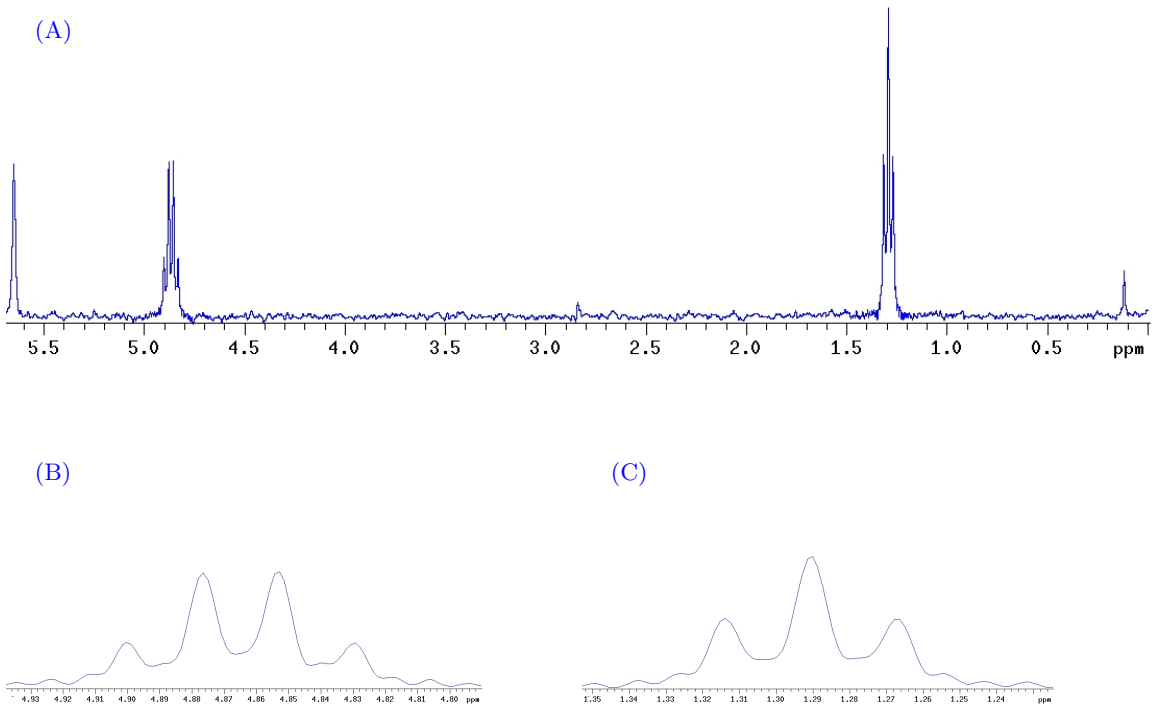

Figure 10.9: Panel (A) shows the full spectrum of the example metabolite, ethyl ether. The metabolite resonance, Panels (B) and (C), are described in the in the Example.ISO file. Metabolites must predict the fractional intensities of the metabolite resonances. Here that means the example subroutine imposes the condition that the area of the quartet should be 2/5 while the area of the triplet should be 3/5.

10.5 Outputs From The Bayes Metabolite Package

The Text outputs files from the Metabolite packages consist of: "Bayes.prob.model," "BayesMetabolite.mcmc.values," "Bayes.params," "Console.log," "Bayes.accepted" and a "Bayes.Condensed.File." These output files can be viewed using the Text Viewer or they can be viewed using File Viewer by navigating to the current working directory and then selecting the files. The format of the mcmc.values report is discussed in Appendix D and the other reports are discussed in Chapter **??**. Additionally, the "Plot Results Viewer" can be used to view the output probability density functions. In addition to the standard data, model and residual plots there are probability density functions for each metabolic parameter and for each frequency, J coupling constant, and decay rate constant in the model. Finally there is probability density functions for the standard deviation of the noise in the time domain Fid data.

Bibliography

[1] Rev. Thomas Bayes (1763), "An Essay Toward Solving a Problem in the Doctrine of Chances," *Philos. Trans. R. Soc. London*, **53,** pp. 370-418; reprinted in *Biometrika*, **45**, pp. 293-315 (1958), and *Facsimiles of Two Papers by Bayes,* with commentary by W. Edwards Deming, New York, Hafner, 1963.

[2] G. Larry Bretthorst (1988), "Bayesian Spectrum Analysis and Parameter Estimation," in *Lecture Notes in Statistics,* **48**, J. Berger, S. Fienberg, J. Gani, K. Krickenberg, and B. Singer (eds), Springer-Verlag, New York, New York.

[3] G. Larry Bretthorst (1990), "An Introduction to Parameter Estimation Using Bayesian Probability Theory," in *Maximum Entropy and Bayesian Methods,* Dartmouth College 1989, P. Fougère *ed.,* pp. 53-79, Kluwer Academic Publishers, Dordrecht the Netherlands.

[4] G. Larry Bretthorst (1990), "Bayesian Analysis I. Parameter Estimation Using Quadrature NMR Models" *J. Magn. Reson.*, **88**, pp. 533-551.

[5] G. Larry Bretthorst (1990), "Bayesian Analysis II. Signal Detection And Model Selection" *J. Magn. Reson.*, **88**, pp. 552-570.

[6] G. Larry Bretthorst (1990), "Bayesian Analysis III. Examples Relevant to NMR" *J. Magn. Reson.*, **88**, pp. 571-595.

[7] G. Larry Bretthorst (1991), "Bayesian Analysis. IV. Noise and Computing Time Considerations," *J. Magn. Reson.*, **93**, pp. 369-394.

[8] G. Larry Bretthorst (1992), "Bayesian Analysis. V. Amplitude Estimation for Multiple Well-Separated Sinusoids," *J. Magn. Reson.*, **98**, pp. 501-523.

[9] G. Larry Bretthorst (1992), "Estimating The Ratio Of Two Amplitudes In Nuclear Magnetic Resonance Data," in *Maximum Entropy and Bayesian Methods,* C. R. Smith *et al.* (eds.), pp. 67-77, Kluwer Academic Publishers, the Netherlands.

[10] G. Larry Bretthorst (1993), "On The Difference In Means," in Physics & Probability Essays in honor of Edwin T. Jaynes, W. T. Grandy and P. W. Milonni (eds.), pp. 177-194, Cambridge University Press, England.

[11] G. Larry Bretthorst (1996), "An Introduction To Model Selection Using Bayesian Probability Theory," in *Maximum Entropy and Bayesian Methods*, G. R. Heidbreder, ed., pp. 1-42, Kluwer Academic Publishers, Printed in the Netherlands.

[12] G. Larry Bretthorst (1999), "The Near-Irrelevance of Sampling Frequency Distributions," in *Maximum Entropy and Bayesian Methods,* W. von der Linden *et al.* (eds.), pp. 21-46, Kluwer Academic Publishers, the Netherlands.

[13] G. Larry Bretthorst (2001), "Nonuniform Sampling: Bandwidth and Aliasing," in *Maximum Entropy and Bayesian Methods in Science and Engineering,* Joshua Rychert, Gary Erickson and C. Ray Smith *eds.*, pp. 1-28, American Institute of Physics, USA.

[14] G. Larry Bretthorst, Christopher D. Kroenke, and Jeffrey J. Neil (2004), "Characterizing Water Diffusion In Fixed Baboon Brain," in Bayesian Inference And Maximum Entropy Methods In Science And Engineering, Rainer Fischer, Roland Preuss and Udo von Toussaint *eds.*, AIP conference Proceedings, **735**, pp. 3-15.

[15] G. Larry Bretthorst, William C. Hutton, Joel R. Garbow, and Joseph J.H. Ackerman (2005), "Exponential parameter estimation (in NMR) using Bayesian probability theory," *Concepts in Magnetic Resonance*, 27A, Issue 2, pp. 55-63.

[16] G. Larry Bretthorst, William C. Hutton, Joel R. Garbow, and Joseph J. H. Ackerman (2005), "Exponential model selection (in NMR) using Bayesian probability theory," *Concepts in Magnetic Resonance*, 27A, Issue 2, pp. 64-72.

[17] G. Larry Bretthorst, William C. Hutton, Joel R. Garbow, and Joseph J.H. Ackerman (2005), "How accurately can parameters from exponential models be estimated? A Bayesian view," *Concepts in Magnetic Resonance*, 27A, Issue 2, pp. 73-83.

[18] G. Larry Bretthorst, W. C. Hutton, J. R. Garbow, and Joseph J. H. Ackerman (2008), "High Dynamic Range MRS Time-Domain Signal Analysis," *Magn. Reson. in Med.*, **62**, pp. 1026-1035.

[19] V. Chandramouli, K. Ekberg, W. C. Schumann, S. C. Kalhan, J. Wahren, and B. R. Landau (1997), "Quantifying gluconeogenesis during fasting," *American Journal of Physiology*, **273**, pp. H1209-H1215.

[20] R. T. Cox (1961), "The Algebra of Probable Inference," Johns Hopkins Univ. Press, Baltimore.

[21] André d'Avignon, G. Larry Bretthorst, Marilyn Emerson Holtzer, and Alfred Holtzer (1998), "Site-Specific Thermodynamics and Kinetics of a Coiled-Coil Transition by Spin Inversion Transfer NMR," *Biophysical Journal*, **74**, pp. 3190-3197.

[22] André d'Avignon, G. Larry Bretthorst, Marilyn Emerson Holtzer, and Alfred Holtzer (1999), "Thermodynamics and Kinetics of a Folded-Folded Transition at Valine-9 of a GCN4-Like Leucine Zipper," *Biophysical Journal*, **76**, pp. 2752-2759.

[23] David Freedman, and Persi Diaconis (1981), "On the histogram as a density estimator: L_2 theory," *Zeitschrift f¨r Wahrscheinlichkeitstheorie und verwandte Gebiete*, **57**, 4, pp. 453-476.

[24] W. R. Gilks, S. Richardson, and D. J. Spiegelhalter (1996), "Markov Chain Monte Carlo in Practice," Chapman & Hall, London.

[25] Paul M. Goggans, and Ying Chi (2004), "Using Thermodynamic Integration to Calculate the Posterior Probability in Bayesian Model Selection Problems," in *Bayesian Inference and Maximum Entropy Methods in Science and Engineering: 23rd International Workshop*, **707**, pp. 59-66.

[26] Marilyn Emerson Holtzer, G. Larry Bretthorst, D. André d'Avignon, Ruth Hogue Angelette, Lisa Mints, and Alfred Holtzer (2001), "Temperature Dependence of the Folding and Unfolding Kinetics of the GCN4 Leucine Lipper via 13C alpha-NMR," *Biophysical Journal*, **80**, pp. 939-951.

[27] E. T. Jaynes (1968), "Prior Probabilities," *IEEE Transactions on Systems Science and Cybernetics*, SSC-4, pp. 227-241; reprinted in [30].

[28] E. T. Jaynes (1978), "Where Do We Stand On Maximum Entropy?" in *The Maximum Entropy Formalism*, R. D. Levine and M. Tribus *Eds.*, pp. 15-118, Cambridge: MIT Press, Reprinted in [30].

[29] E. T. Jaynes (1980), "Marginalization and Prior Probabilities," in *Bayesian Analysis in Econometrics and Statistics*, A. Zellner *ed.,* North-Holland Publishing Company, Amsterdam; reprinted in [30].

[30] E. T. Jaynes (1983), "Papers on Probability, Statistics and Statistical Physics," a reprint collection, D. Reidel, Dordrecht the Netherlands; second edition Kluwer Academic Publishers, Dordrecht the Netherlands, 1989.

[31] E. T. Jaynes (1957), "How Does the Brain do Plausible Reasoning?" unpublished Stanford University Microwave Laboratory Report No. 421; reprinted in *Maximum-Entropy and Bayesian Methods in Science and Engineering* **1,** pp. 1-24, G. J. Erickson and C. R. Smith *Eds.,* 1988.

[32] E. T. Jaynes (2003), "Probability Theory—The Logic of Science," edited by G. Larry Bretthorst, Cambridge University Press, Cambridge UK.

[33] Sir Harold Jeffreys (1939), "Theory of Probability," Oxford Univ. Press, London; Later editions, 1948, 1961.

[34] John G. Jones, Michael A. Solomon, Suzanne M. Cole, A. Dean Sherry, and Craig R. Malloy (2001) "An integrated ^{2}H and ^{13}C NMR study of gluconeogenesis and TCA cycle flux in humans," *American Journal of Physiology, Endocrinology, and Metabolism,* **281,** pp. H848-H856.

[35] John Kotyk, N. G. Hoffman, W. C. Hutton, G. Larry Bretthorst, and J. J. H. Ackerman (1992), "Comparison of Fourier and Bayesian Analysis of NMR Signals. I. Well-Separated Resonances (The Single-Frequency Case)," *J. Magn. Reson.*, **98**, pp. 483–500.

[36] Pierre Simon Laplace (1814), "A Philosophical Essay on Probabilities," John Wiley & Sons, London, Chapman & Hall, Limited 1902. Translated from the 6th edition by F. W. Truscott and F. L. Emory.

[37] N. Lartillot, and H. Philippe (2006), "Computing Bayes Factors Using Thermodynamic Integration," *Systematic Biology*, **55** (2), pp. 195-207.

[38] D. Le Bihan, and E. Breton (1985), "Imagerie de diffusion in-vivo par rsonance," Comptes rendus de l'Acadmie des Sciences (Paris), **301** (15), pp. 1109-1112.

[39] N. R. Lomb (1976), "Least-Squares Frequency Analysis of Unevenly Spaced Data," *Astrophysical and Space Science*, **39**, pp. 447-462.

[40] T. J. Loredo (1990), "From Laplace To SN 1987A: Bayesian Inference In Astrophysics," in *Maximum Entropy and Bayesian Methods,* P. F. Fougere (ed), Kluwer Academic Publishers, Dordrecht, The Netherlands.

[41] Craig R. Malloy, A. Dean Sherry, and Mark Jeffrey (1988), "Evaluation of Carbon Flux and Substrate Selection through Alternate Pathways Involving the Citric Acid Cycle of the Heart by 13C NMR Spectroscopy," *Journal of Biological Chemistry*, **263** (15), pp. 6964-6971.

[42] Craig R. Malloy, Dean Sherry, and Mark Jeffrey (1990), "Analysis of tricarboxylic acid cycle of the heart using ^{13}C isotope isomers," *American Journal of Physiology*, **259**, pp. H987-H995.

[43] Lawrence R. Mead and Nikos Papanicolaou, "Maximum entropy in the problem of moments," *J. Math. Phys.* **25**, 2404–2417 (1984).

[44] K. Merboldt, Wolfgang Hanicke, and Jens Frahm (1969), "Self-diffusion NMR imaging using stimulated echoes," Journal of Magnetic Resonance, **64** (3), pp. 479-486.

[45] Nicholas Metropolis, Arianna W. Rosenbluth, Marshall N. Rosenbluth, Augusta H. Teller, and Edward Teller (1953), "Equation of State Calculations by Fast Computing Machines," Journal of Chemical Physics. The previous link is to the Americain Institute of Physics and if you do not have access to Science Sitations you many not be able to retrieve this paper.

[46] Radford M. Neal (1993), "Probabilistic Inference Using Markov Chain Monte Carlo Methods," technical report CRG-TR-93-1, Dept. of Computer Science, University of Toronto.

[47] Jeffrey J. Neil, and G. Larry Bretthorst (1993), "On the Use of Bayesian Probability Theory for Analysis of Exponential Decay Data: An Example Taken from Intravoxel Incoherent Motion Experiments," *Magn. Reson. in Med.*, **29**, pp. 642–647.

[48] H. Nyquist (1924), "Certain Factors Affecting Telegraph Speed," *Bell System Technical Journal*, **3**, pp. 324-346.

[49] H. Nyquist (1928), "Certain Topics in Telegraph Transmission Theory," *Transactions AIEE*, **3**, pp. 617-644.

[50] William H. Press, Saul A. Teukolsky, William T. Vetterling and Brian P. Flannery (1992), "Numerical Recipes The Art of Scientific Computing Second Edition," Cambridge University Press, Cambridge UK.

[51] Emanuel Parzen (1962), "On Estimation of a Probability Density Function and Mode," *Annals of Mathematical Statistics* **33**, 1065–1076

[52] Karl Pearson (1895), "Contributions to the Mathematical Theory of Evolution. II. Skew Variation in Homogeneous Material," *Phil. Trans. R. Soc. A* **186**, 343–326.

[53] Murray Rosenblatt, "Remarks on Some Nonparametric Estimates of a Density Function," *Annals of Mathematical Statistics* **27**, 832–837 (1956).

[54] Jeffery D. Scargle (1981), "Studies in Astronomical Time Series Analysis I. Random Process In The Time Domain," *Astrophysical Journal Supplement Series*, **45**, pp. 1-71.

[55] Jeffery D. Scargle (1982), "Studies in Astronomical Time Series Analysis II. Statistical Aspects of Spectral Analysis of Unevenly Sampled Data," *Astrophysical Journal*, **263**, pp. 835-853.

[56] Jeffery D. Scargle (1989), "Studies in Astronomical Time Series Analysis. III. Fourier Transforms, Autocorrelation Functions, and Cross-correlation Functions of Unevenly Spaced Data," *Astrophysical Journal*, **343**, pp. 874-887.

[57] Arthur Schuster (1905), "The Periodogram and its Optical Analogy," *Proceedings of the Royal Society of London*, **77**, p. 136-140.

[58] Claude E. Shannon (1948), "A Mathematical Theory of Communication," *Bell Syst. Tech. J.*, **27**, pp. 379-423.

[59] John E. Shore, and Rodney W. Johnson (1981), "Properties of cross-entropy minimization," *IEEE Trans. on Information Theory*, **IT-27,** No. 4, pp. 472-482.

[60] John E. Shore and Rodney W. Johnson (1980), "Axiomatic derivation of the principle of maximum entropy and the principle of minimum cross-entropy," *IEEE Trans. on Information Theory*, **IT-26** (1), pp. 26-37.

[61] Devinderjit Sivia, and John Skilling (2006), "Data Analysis: A Bayesian Tutorial," Oxford University Press, USA.

[62] Edward O. Stejskal and Tanner, J. E. (1965), "Spin Diffusion Measurements: Spin Echoes in the Presence of a Time-Dependent Field Gradient." Journal of Chemical Physics, **42** (1), pp. 288-292.

[63] D. G. Taylor and Bushell, M. C. (1985), "The spatial mapping of translational diffusion coefficients by the NMR imaging technique," Physics in Medicine and Biology, **30** (4), pp. 345-349.

[64] Myron Tribus (1969), "Rational Descriptions, Decisions and Designs," Pergamon Press, Oxford.

[65] P. M. Woodward (1953), "Probability and Information Theory, with Applications to Radar," McGraw-Hill, N. Y. Second edition (1987); R. E. Krieger Pub. Co., Malabar, Florida.

[66] Arnold Zellner (1971), "An Introduction to Bayesian Inference in Econometrics," John Wiley and Sons, New York.

Index